

# Game-Theoretic Modeling of Multi-Vehicle Interactions at Uncontrolled Intersections

Nan Li<sup>ID</sup>, Member, IEEE, Yu Yao<sup>ID</sup>, Member, IEEE, Ilya Kolmanovsky<sup>ID</sup>, Fellow, IEEE,  
Ella Atkins<sup>ID</sup>, Senior Member, IEEE, and Anouck R. Girard<sup>ID</sup>, Senior Member, IEEE

**Abstract**—Motivated by the need for simulation tools for testing, verification and validation of autonomous driving systems that operate in traffic consisting of both autonomous and human-driven vehicles, we propose a game-theoretic framework for modeling the interactive behavior of vehicles at uncontrolled intersections. The proposed vehicle interaction model is based on a novel formulation of dynamic games with multiple concurrent leader-follower pairs, induced from common traffic rules. Based on simulation results for various intersection scenarios, we show that the model exhibits reasonable behavior expected in traffic, including the capability of reproducing scenarios extracted from real-world traffic data and reasonable performance in resolving traffic conflicts. The model is further validated based on the level-of-service traffic quality rating system and demonstrates manageable computational complexity compared to traditional multi-player game-theoretic models.

**Index Terms**—Autonomous vehicles, decision making, game theory, human factors, multi-agent systems, vehicle safety.

## I. INTRODUCTION

TO PROVIDE safer, cleaner and more efficient transportation is the promise of autonomous driving technologies [1]. Thanks to the extensive efforts that have been made in both academia and industry to pursue this goal, advances in perception, decision-making/planning, control theory and computing systems have made fully autonomous driving possible [2]. However, before autonomous vehicles can be deployed in mass production, their control systems need to be verified to have promised safety and liveness performance when operating in various traffic environments, which remains a challenging problem [3]. On the one hand, simulation tools can be used for quick and safe virtual testing of these systems and to reduce the time and cost of road tests. On the other hand, the reliability of virtual testing results depends on the fidelity of the simulations in terms of modeling real-world traffic scenarios.

In the near to medium term, autonomous vehicles will likely operate in traffic scenarios together with human-driven

Manuscript received April 9, 2019; revised November 26, 2019 and July 13, 2020; accepted September 8, 2020. Date of publication October 6, 2020; date of current version February 2, 2022. This work was supported by the National Science Foundation under Award CNS 1544844. The Associate Editor for this article was N. Geroliminis. (*Corresponding author: Nan Li*)

Nan Li, Ilya Kolmanovsky, and Anouck R. Girard are with the Department of Aerospace Engineering, University of Michigan, Ann Arbor, MI 48109 USA (e-mail: nanli@umich.edu; ilya@umich.edu; anouck@umich.edu).

Yu Yao and Ella Atkins are with the Robotics Institute, University of Michigan, Ann Arbor, MI 48109 USA (e-mail: brianyao@umich.edu; ematkins@umich.edu).

Digital Object Identifier 10.1109/TITS.2020.3026160

vehicles, where interactions between autonomous vehicles and human-driven vehicles will constantly occur. Among different traffic scenarios, the interactive behavior of vehicles at intersections may be particularly complex. An autonomous driving system must account for these interactions to be able to operate safely and effectively at an intersection.

By types of traffic control, intersections can be classified as signal-controlled, “stop” or “yield” sign-controlled, and uncontrolled [4]. Uncontrolled intersections are intersections without traffic signals or signs, and are common in both urban and rural settings over the world [5]–[7]. According to the U.S. National Highway Traffic Safety Administration’s fatality analysis report, more than one fourth of fatal crashes in the U.S. occur at or are related to intersections, and about 50% of these occur at uncontrolled intersections [8].

At an uncontrolled intersection, due to the lack of guidance from traffic signals or signs, drivers/automations need to decide whether, when and how to enter and pass through the intersection on their own. In this case, accounting for the interactions among vehicles is particularly important: Failures in accounting for these interactions may cause deadlocks if driving overly conservatively – the vehicles may get stuck and never pass through the intersection, or may cause collisions if driving overly aggressively.

Advanced strategies that have been proposed for handling vehicle interactions at intersections include cooperative driving, where vehicles cooperate with each other and with road infrastructure to resolve traffic conflicts. They may cooperate through vehicle-to-vehicle negotiations [9]–[11], or through coordination by a centralized traffic “manager” in the approach called “autonomous intersection management” [12]–[14]. Although strategies based on cooperative driving have been shown to be capable of improving intersection traffic safety and efficiency, they rely on dense penetration of vehicle-to-vehicle and/or vehicle-to-infrastructure communications as well as autonomous driving systems, which will likely not be the case in the near to medium term.

Alternative strategies have been focused on individual control of the autonomous ego vehicle. To account for the interactions among vehicles, strategies based on online verification using reachability analysis [15], [16], receding-horizon optimization [17], [18], learning [19] and game theory [20]–[24], have been proposed. Although these approaches have established the theoretical foundations of creating autonomous driving systems that are capable of handling

vehicle interactions at uncontrolled intersections, they must be tested and calibrated to achieve promised safety and liveness performance.

Simulation tools used for virtual testing of these control systems are supposed to be capable of representing the interactive behavior of vehicles with reasonable fidelity, which motivates the development of vehicle interaction models. In this article, we propose such a model for uncontrolled intersections based on a novel game-theoretic formulation. This model is intended for control system testing and verification, and not for operating actual vehicles in real traffic.

Game theory is a useful tool for modeling the strategic interactions between intelligent decision-makers (such as drivers, in the setting of this article) [25], and has been exploited by several researchers for modeling the interactive behavior of vehicles in traffic. For instance, in [20], the vehicle-to-vehicle interactions at an intersection are modeled using normal-form games – vehicles select actions between “Stop” and “Go” according to their payoff matrices. However, the performance of the approach in [20] is limited due to the limited number of action choices (i.e., two) and the fact that the dynamic behavior of the vehicles is not explicitly taken into account when the payoff matrices are designed. In particular, as the number of interacting vehicles increases to 6, almost half of the simulation runs following the approach of [20] lead to deadlocks. In [21], the interactions between an autonomous vehicle and a human-driven vehicle are modeled based on the formulation of a two-player game, where vehicle dynamics are explicitly accounted for. The results of an intersection scenario with two interacting vehicles, both driving straight to cross the intersection, are reported. Extensions of this approach to traffic scenarios with more interacting vehicles have not been reported and may not be straightforward due to both theoretical limitations and computational challenges [21].

In our previous work [26]–[28], a game-theoretic framework for modeling vehicle-to-vehicle interactions in multi-vehicle highway traffic scenarios has been proposed. The framework is based on the application of level-k game theory [29], [30] and explicitly takes into account the dynamic behavior of the vehicles. The vehicle driving policies are determined using reinforcement learning. Once the policies have been obtained offline, highway scenarios with a possibly large number of interacting vehicles can be modeled with minimum online computational effort. Such a level-k game-theoretic framework has also been extended to model the interactions between two vehicles at an uncontrolled four-way intersection in [31] and at a roundabout intersection in [32].

The contributions of the present paper are: 1) We propose a framework based on a novel formulation of dynamic games with multiple concurrent leader-follower pairs (thus, different from our previous level-k framework) and receding-horizon optimization for modeling the interactive behavior of vehicles at uncontrolled intersections. The framework explicitly accounts for the dynamic behavior of the vehicles and common traffic rules. It is generalizable to traffic scenarios with more than 2 interacting vehicles (results with up to 10 vehicles are reported). 2) The framework is applied to a parameterized intersection model so that interactive traffic in various

uncontrolled intersection scenarios (with various numbers of interacting vehicles, intersection layouts and geometries, etc) can be modeled and simulated. 3) Based on simulation and statistical evaluation results, we show that the model exhibits reasonable behavior expected in traffic. In particular, it can reproduce scenarios extracted from real-world traffic data, and has reasonable performance in resolving traffic conflicts in complex intersection scenarios and when interacting with different driver models. Furthermore, the model demonstrates a manageable increase in computational complexity as the number of interacting vehicles increases.

This article is organized as follows: In Section II, we describe our novel game-theoretic approach to modeling the interactive decision-making processes of drivers/vehicles at uncontrolled intersections. In Section III, we describe the integration of the decision-making model in Section II and a parameterized intersection model, including descriptions of our kinematics model to represent the vehicles’ dynamic behavior and our reward function design to represent drivers’ decision-making objectives. In Section IV, we incorporate several additional considerations in our model to improve the fidelity of our model in imitating the decision-making processes of human drivers. In Section V, we consider multiple simulation case studies to comprehensively illustrate and evaluate our proposed framework for modeling vehicle interactions at uncontrolled intersections. The paper is summarized and concluded in Section VI.

## II. VEHICLE INTERACTIVE DECISION-MAKING BASED ON LEADER-FOLLOWER GAME

In this section, we introduce our approach to modeling the interactive decision-making processes of drivers/vehicles at uncontrolled intersections based on a novel game-theoretic formulation with multiple concurrent leader-follower pairs. We first describe the logic for assigning pairwise leader/follower roles to the vehicles at an uncontrolled intersection in Section II-A, which is the foundation for formulating our leader-follower game. We then describe our decision-making models for the pairwise leader and follower in the setting of two-vehicle interactions in Section II-B, and extend them to the setting of multiple-vehicle interactions in Section II-C.

### A. Leader-Follower Role Assignment

Human drivers resolve their conflicts when interacting at uncontrolled intersections typically through following the “right-of-way” rules [33]. The right-of-way rules help the drivers decide who should proceed first to pass through the intersection. Motivated by the right-of-way rules, we assign a leader-follower relationship to each pair of vehicles (denoted by  $(i, j)$ ) at an intersection based on the following logic:

- (1) If vehicles  $i, j$  have both entered the intersection, the vehicle with a strictly smaller signed distance to the exit of the intersection is the leader.
- (2) If at most one of vehicles  $i, j$  has entered the intersection, the vehicle with a strictly smaller signed distance to the entrance of the intersection is the leader.

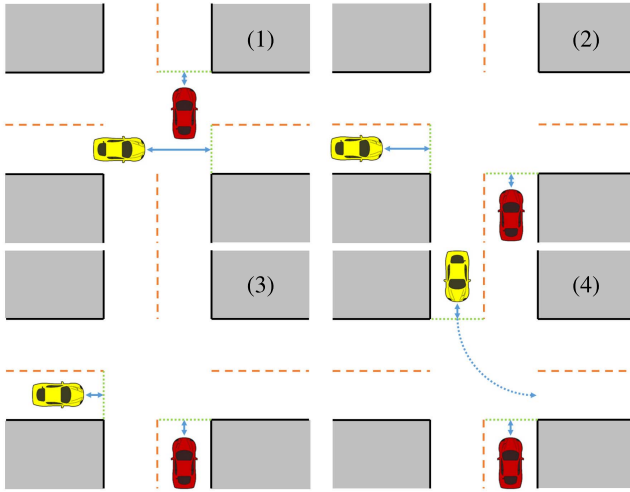


Fig. 1. Leader-follower role assignment. In all of the figures, the red car is the leader and the yellow car is the follower.

- (3) If no leader has been assigned to  $(i, j)$  according to (1)-(2), then the vehicle on the right is the leader when the two vehicles are coming from adjacent road arms.
- (4) If no leader has been assigned to  $(i, j)$  according to (1)-(3), then the vehicle going straight is the leader when the other vehicle is making a turn.

The above leader-follower role assignment logic is also illustrated in Fig. 1. We note that if a vehicle has entered (exited) the intersection, then its signed distance to the entrance (exit) of the intersection is the negative of the corresponding distance.

If vehicle  $i$  is the leader in the pair  $(i, j)$ , we write  $i \prec j$ ; if  $i$  is not the leader (i.e., either  $j$  is the leader or no leader is determined between  $i$  and  $j$  according to (1)-(4)), we write  $i \succeq j$ .

We note that  $\prec$  and  $\succeq$  do not have the transitive property:  $i \prec j$  and  $j \prec k$  ( $i \succeq j$  and  $j \succeq k$ ) do not imply  $i \prec k$  ( $i \succeq k$ ). This can be seen by considering the traffic scenario where four vehicles  $i, j, k$  and  $l$  coming from different road arms arrive at the entrances of a four-way intersection at the same time. Then, based on the above role assignment logic we have  $i \prec j, j \prec k, k \prec l$  and  $l \prec i$ . Indeed, this scenario and similar scenarios where such a cyclic pattern occurs are challenging scenarios for both human drivers and autonomous vehicles – they may cause deadlocks, i.e., no one decides to enter the intersection or everyone gets stuck in the middle of the intersection.

The above logic, integrated with our parameterized intersection and vehicle kinematics models as well as the practical consideration of perception imperfections, is rephrased in formal language as Algorithm 1 in Section III-B.

### B. Leader-Follower Based Decision-Making in Two-Vehicle Interactions

Once the leader-follower relationship between the pair of vehicles  $(i, j)$  has been determined, we describe our model for representing their interactive decision-making processes.

Let  $\gamma_l (\gamma_f)$  denote an action of the leader (follower), taking values in an action set  $\Gamma_l (\Gamma_f)$ . Either player makes decisions on its action choices to maximize a reward function, denoted by  $\mathbb{R}_l(\mathbf{s}, \gamma_l, \gamma_f)$  for the leader and by  $\mathbb{R}_f(\mathbf{s}, \gamma_l, \gamma_f)$  for the follower, where  $\mathbf{s} \in \mathcal{S}$  denotes the present state in which the two players are making their decisions. In particular, when modeling two-vehicle interactions,  $\mathbf{s}$  contains the states of these two vehicles, i.e.,  $\mathbf{s} = (s_i, s_j)$  with  $s_i (s_j)$  denoting the state of vehicle  $i$  (vehicle  $j$ ). We note that the precise interpretations of the states and actions are coupled with our parameterized intersection and vehicle kinematics models specifically used in this article, and will be introduced in Section III-B. We also note that the dependence of either player's reward on both players' states and actions reflects the interactive nature of such a decision-making process.

Specifically, we let the leader and the follower make decisions according to, respectively, (1) and (2):

$$\gamma_l^*(\mathbf{s}) \in \arg \max_{\gamma_l \in \Gamma_l} \mathbb{Q}_l(\mathbf{s}, \gamma_l), \quad (1)$$

$$\gamma_f^*(\mathbf{s}) \in \arg \max_{\gamma_f \in \Gamma_f} \mathbb{Q}_f(\mathbf{s}, \gamma_f), \quad (2)$$

where the functions  $\mathbb{Q}_l$  and  $\mathbb{Q}_f$  are defined as

$$\begin{aligned} \mathbb{Q}_l(\mathbf{s}, \gamma_l) &:= \min_{\gamma_f \in \Gamma_f^*(\mathbf{s})} \mathbb{R}_l(\mathbf{s}, \gamma_l, \gamma_f), \\ \mathbb{Q}_f(\mathbf{s}, \gamma_f) &:= \min_{\gamma_l \in \Gamma_l} \mathbb{R}_f(\mathbf{s}, \gamma_l, \gamma_f), \end{aligned} \quad (3)$$

with

$$\Gamma_f^*(\mathbf{s}) := \{\gamma'_f \in \Gamma_f : \mathbb{Q}_f(\mathbf{s}, \gamma'_f) \geq \mathbb{Q}_f(\mathbf{s}, \gamma_f), \forall \gamma_f \in \Gamma_f\}. \quad (4)$$

The above decision-making processes for the leader and the follower can be explained as follows: Firstly, according to the role assignment criterion introduced in Section II-A, the pairwise leader corresponds to a vehicle that typically has the right of way in real-world intersection scenarios, and in turn, the pairwise follower should yield to the leader. On the one hand, considering the facts that 1) the two vehicles make simultaneous decisions at each time instant, 2) the follower cannot instantaneously respond to the leader's immediate decision due to, e.g., reaction delay, and 3) as a result, the follower has to make its decision only based on the current states of the two vehicles, we let the follower make a conservative decision by maximizing the worst-case reward in (2), called a *maximin* strategy. On the other hand, we assume the leader knows that the follower should yield and will in such a case apply a conservative maximin strategy to secure its rewards. With such knowledge, the leader can predict the follower's decision and make an optimal response according to (1).

We note that the above leader-follower based decision-making model is partly inspired by a similar philosophy as in the Stackelberg game theory [34]. Specifically, by granting the leader some advantages over the follower in the decision-making model, it is possible to represent certain superior aspects of one side over the other in real-world competitive situations. In particular, the advantage that we grant to the leader is the awareness of the follower's maximin strategy and the corresponding capability of predicting the follower's decisions, and the superior aspect of the leader vehicle that

we represent is the possession of right of way in intersection scenarios. Note that we do not adopt a standard Stackelberg equilibrium based decision-making model because a Stackelberg model relies on several stronger assumptions, such as the follower must be able to observe and instantaneously respond to the leader's immediate decision and the leader must know this *ex-ante* [35], which generally may not hold in the setting of driver/vehicle interactions in traffic due to, for instance, driver reaction delay [36].

After making the following technical assumptions on the uniqueness of maximizers,

$$\begin{aligned} \forall (\mathbf{s}, \gamma_f) \in \mathbf{S} \times \Gamma_f, \exists! \gamma'_l \in \Gamma_l \text{ such that} \\ \mathbb{R}_l(\mathbf{s}, \gamma'_l, \gamma_f) \geq \mathbb{R}_l(\mathbf{s}, \gamma_l, \gamma_f), \forall \gamma_l \in \Gamma_l; \\ \forall \mathbf{s} \in \mathbf{S}, \exists! \gamma'_f \in \Gamma_f \text{ such that} \\ \min_{\gamma_l \in \Gamma_l} \mathbb{R}_f(\mathbf{s}, \gamma_l, \gamma'_f) \geq \min_{\gamma_l \in \Gamma_l} \mathbb{R}_f(\mathbf{s}, \gamma_l, \gamma_f), \forall \gamma_f \in \Gamma_f, \quad (5) \end{aligned}$$

the decision-making model (1)-(4) can be simplified to

$$\begin{aligned} \gamma_l^*(\mathbf{s}) &= \arg \max_{\gamma_l \in \Gamma_l} \mathbb{Q}_l(\mathbf{s}, \gamma_l), \\ \gamma_f^*(\mathbf{s}) &= \arg \max_{\gamma_f \in \Gamma_f} \mathbb{Q}_f(\mathbf{s}, \gamma_f), \\ \mathbb{Q}_l(\mathbf{s}, \gamma_l) &= \mathbb{R}_l(\mathbf{s}, \gamma_l, \gamma_f^*(\mathbf{s})), \\ \mathbb{Q}_f(\mathbf{s}, \gamma_f) &= \min_{\gamma_l \in \Gamma_l} \mathbb{R}_f(\mathbf{s}, \gamma_l, \gamma_f). \quad (6) \end{aligned}$$

Assumption (5) means that at each traffic state  $\mathbf{s}$ , for either player ( $l$  or  $f$ ), there is one action that is strictly better than the others to choose. We note that based on our reward function design in Section III-C, this assumption holds.

### C. Pairwise Leader-Follower Based Decision-Making in Multi-Vehicle Interactions

We now extend the decision-making model (6) representing two-vehicle interactions to the setting of  $n$ -vehicle interactions with  $n \geq 2$ . Although 2-player leader-follower games may be extended to  $n$ -player games through considering a multi-level decision-making hierarchy, e.g., player  $k$  being the leader of players  $k+1, \dots, n$  and being the follower of players  $1, \dots, k-1$  for every  $k \in \{1, \dots, n\}$ , or allowing a level to accommodate multiple players, e.g., players  $2, \dots, n$  being the followers of player 1 and applying Nash equilibrium-based strategies among themselves, such generalizations require exponentially increasing computational efforts to solve for solutions as the number of players increases. For instance, a Stackelberg equilibrium solution can be difficult to compute when  $n > 3$  [37]. In contrast, the extended model described in this section is computationally scalable, which is crucial to the practical application of the framework to modeling complex intersection scenarios with a possibly medium to large number of traffic participants.

Our extension relies on the pairwise leader-follower relationships defined for all vehicle pairs at an intersection, and the decision-making process of every single vehicle accounts for all of the pairwise leader-follower relationships related to itself. In particular, we let vehicle  $i$ , for  $i = 1, 2, \dots, n$ , make

decisions on its action choices according to:

$$\begin{aligned} \gamma_i^*(\mathbf{s}_{\text{traffic}}) &\in \arg \max_{\gamma_i \in \Gamma_i} \underline{\mathbb{Q}}_i(\mathbf{s}_{\text{traffic}}, \gamma_i), \\ \underline{\mathbb{Q}}_i(\mathbf{s}_{\text{traffic}}, \gamma_i) &:= \min_{j \in \{1, \dots, n\}, j \neq i} \mathbb{Q}_{i,j}(\mathbf{s}_{i,j}, \gamma_i), \\ \mathbb{Q}_{i,j}(\mathbf{s}_{i,j}, \gamma_i) &:= \begin{cases} \mathbb{Q}_l(\mathbf{s}_{i,j}, \gamma_i) & \text{if } i < j, \\ \mathbb{Q}_f(\mathbf{s}_{i,j}, \gamma_i) & \text{if } i \geq j, \end{cases} \quad (7) \end{aligned}$$

where  $\mathbb{Q}_l(\mathbf{s}_{i,j}, \gamma_i)$  ( $\mathbb{Q}_f(\mathbf{s}_{i,j}, \gamma_i)$ ) is defined in (6) with player  $i$  being the leader  $l$  (the follower  $f$ ); the traffic state  $\mathbf{s}_{\text{traffic}}$  contains now the states of all interacting vehicles at the intersection, i.e.,  $\mathbf{s}_{\text{traffic}} = (s_1, \dots, s_n)$ ; and  $\mathbf{s}_{i,j} = (s_i, s_j)$  represents the state of the vehicle pair  $(i, j)$ .

The decision-making model (7) can be interpreted as follows: If  $i$  is the follower of  $j$  ( $i \geq j$ ), the secured reward of action  $\gamma_i$  is the least reward  $i$  may get due to the uncertain action choice of  $j$ ; if  $i$  is the leader of  $j$  ( $i < j$ ),  $i$  knows that the most aggressive action that  $j$  can choose is subject to  $j$ 's maximin principle between their pairwise interactions, and thus  $i$  predicts the reward of action  $\gamma_i$  by assuming  $j$  to apply its maximin action of their pair. On top of this, to account for its interactions with all of the other players,  $i$  maximizes the minimum of its secured/predicted rewards over all pairwise interactions. We will show through multiple simulation case studies in Section V that the model (7) can generate realistic vehicle interaction behaviors, has satisfactory performance in terms of safety (not overly aggressive, represented by reasonable collision rates) and liveness (not overly conservative, represented by reasonable deadlock rates), and also demonstrates manageable computational complexity.

## III. INTERSECTION AND VEHICLE MODELING

Simulation tools used for verification and validation of autonomous vehicles are supposed to cover a sufficiently rich set of traffic scenarios. For instance, intersections in real-world road networks can have various layouts (e.g., number of road arms) and geometries (e.g., angles between road arms and lane width). To enable our framework to model the interactive behavior of vehicles at these intersections, in this section we first introduce briefly a parameterized intersection model and then describe the integration of our decision-making model in Section II with this intersection model, including descriptions of our kinematics model to represent the vehicles' dynamic behavior and our reward function design to represent drivers' decision-making objectives.

### A. Parameterized Intersection

We characterize the layout and geometry of an intersection using the following set of parameters,

$$(N, \{M_f^{(m)}\}_{m=1}^N, \{M_b^{(m)}\}_{m=1}^N, \{\phi^{(m)}\}_{m=1}^N, w_{\text{lane}}), \quad (8)$$

where  $N \in \{3, 4, 5\}$  denotes the number of road arms,  $M_f^{(m)} \in \{0, 1, 2, \dots\}$  and  $M_b^{(m)} \in \{0, 1, 2, \dots\}$  denote, respectively, the numbers of forward and backward lanes<sup>1</sup> of the  $m$ th arm,

<sup>1</sup>A forward lane (a backward lane) is a lane for traffic entering the intersection (moving away from the intersection).

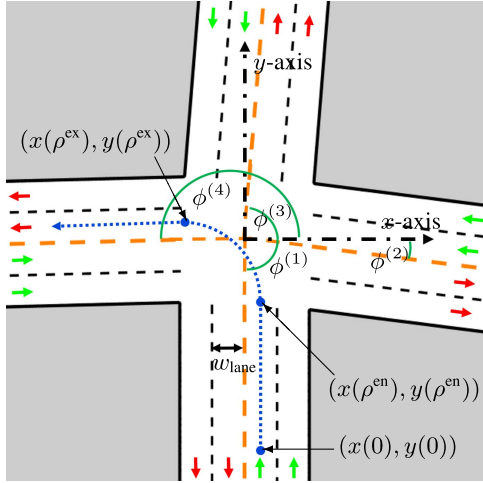


Fig. 2. A four-way intersection modeled by (8) and (9). The orange dashed lines are the road centerlines<sup>3</sup>, the black dashed lines are the lane markings that separate the lanes of traffic moving in the same directions, the black solid lines are the road boundaries, and the shaded polygons are off-road regions.

$\phi^{(m)}$  is the counter-clockwise angle of the  $m$ th arm with respect to the  $x$ -axis, and  $w_{\text{lane}}$  is the lane width.<sup>2</sup> We consider three-, four- and five-way intersections ( $N \in \{3, 4, 5\}$ ) as they are most common in real-world road networks. Note that  $M_f^{(m)} = 0$  or  $M_b^{(m)} = 0$  (but not simultaneously equal to 0) represents one-way roads, which are allowed in our model. We assume that the road centerlines<sup>3</sup> of all the road arms intersect at the same point, which is referred to as the intersection center with coordinates  $(x_0, y_0) = (0, 0)$ .

Given a set of parameters (8), the lane markings and road boundaries of the  $m$ th arm can be determined according to

$$x \sin(\phi^{(m)}) - y \cos(\phi^{(m)}) + \frac{k w_{\text{lane}}}{2} = 0, \quad (9)$$

with  $k \in \{-2M_b^{(m)}, \dots, 2M_f^{(m)}\}$ . When  $k = 2M_f^{(m)}$  (resp.  $k = -2M_b^{(m)}$ ), (9) corresponds to the right-hand-side road boundary when looking in the forward direction (resp. in the backward direction); when  $k \in 2\{M_f^{(m)} - 1, \dots, 1\}$  (resp.  $k \in 2\{-M_b^{(m)} + 1, \dots, -1\}$ ), (9) corresponds to a lane marking that separates two lanes of traffic moving in the forward direction (resp. in the backward direction); when  $k = 0$ , (9) corresponds to the road centerline; and when  $k \in 2\{M_f^{(m)}, \dots, 1\} - 1$  (resp.  $k \in 2\{-M_b^{(m)}, \dots, -1\} + 1$ ), (9) corresponds to the geometric center of a forward lane (resp. backward lane). We also assign an entrance point  $(x(\rho^{\text{en}}), y(\rho^{\text{en}}))$  to each forward lane and an exit point  $(x(\rho^{\text{ex}}), y(\rho^{\text{ex}}))$  to each backward lane, both located in the center of the corresponding lanes and indicating the entrance/exit of the intersection, which will be used when assigning the leader/follower roles to vehicles (see Section II-A).

<sup>2</sup>We assume that all of the lanes have the same width although in principle they do not have to.

<sup>3</sup>The road centerlines are the lane markings that separate the lanes of traffic moving in the opposite directions, not necessarily the centerlines in the geometric sense, e.g., for a road arm with different numbers of forward and backward lanes.

Fig. 2 shows an example of a four-way intersection modeled according to (8) and (9). We note that the parameterized intersection model described above corresponds to the right-hand traffic [38]. To model intersections in the context of left-hand traffic requires straightforward modifications.

### B. Vehicle Kinematics

We represent a vehicle using a rectangle bounding the vehicle's geometric contour projected onto the ground. This rectangle is referred to as the “collision zone” ( $c$ -zone) as an overlap of two vehicles'  $c$ -zones indicates a danger of collision. A 5-tuple  $(x, y, \theta, l_c, w_c)$  is used to characterize the  $c$ -zone of a vehicle, where  $(x, y)$  are the coordinates of its geometric center,  $\theta$  is the vehicle's heading angle (the counter-clockwise angle of the vehicle's heading direction with respect to the  $x$ -axis), and  $l_c (w_c)$  is the length (width) of the rectangle.

We assume that a vehicle plans a path  $\mathcal{P}$  according to its origin lane and target lane<sup>4</sup> before entering the intersection and follows this pre-planned path to pass through the intersection. When there are conflicts between vehicles, they adjust their speeds along the paths correspondingly. Such an assumption is often adopted in the literature [39].

In particular, the path  $\mathcal{P}$  is a smooth curve initialized at an initial point  $(x^{\text{ini}}, y^{\text{ini}})$  located in the center of the vehicle's origin lane, passing through the entrance point  $(x(\rho^{\text{en}}), y(\rho^{\text{en}}))$  of that lane and the exit point  $(x(\rho^{\text{ex}}), y(\rho^{\text{ex}}))$  of the vehicle's target lane, and terminated at a terminal point  $(x^{\text{term}}, y^{\text{term}})$  located in the center of that lane. For any point  $(x, y)$  on the curve, we denote by  $\rho$  the length of the curve segment from  $(x^{\text{ini}}, y^{\text{ini}})$  to  $(x, y)$ . This way,  $(x(0), y(0)) = (x^{\text{ini}}, y^{\text{ini}})$ , i.e., the initial point is the location of the vehicle when its traveled distance along the path is zero. Also, we let  $\rho^{\text{en}}$  (resp.  $\rho^{\text{ex}}$ ) denote the value of  $\rho$  corresponding to the point on  $\mathcal{P}$  with coordinates  $(x(\rho^{\text{en}}), y(\rho^{\text{en}}))$  (resp.  $(x(\rho^{\text{ex}}), y(\rho^{\text{ex}}))$ ),<sup>5</sup> i.e., the vehicle enters (resp. exits) the intersection when its traveled distance along the path is  $\rho^{\text{en}}$  (resp.  $\rho^{\text{ex}}$ ). Then, we define the signed distance of the vehicle to the entrance (resp. exit) of the intersection as  $\Delta\rho^{\text{en}} = \rho^{\text{en}} - \rho$  (resp.  $\Delta\rho^{\text{ex}} = \rho^{\text{ex}} - \rho$ ) so that  $\Delta\rho^{\text{en}} < 0$  (resp.  $\Delta\rho^{\text{ex}} < 0$ ) means that the vehicle has entered (resp. exited) the intersection.

To facilitate following expositions, we write  $\mathcal{P}$  formally as

$$\mathcal{P} : \mathbf{R} \rightarrow \mathbf{R}^2, \quad \rho \mapsto \begin{bmatrix} x(\rho) \\ y(\rho) \end{bmatrix}. \quad (10)$$

We note that analytical expressions for the curve (10) and for  $\Delta\rho^{\text{en}}$  and  $\Delta\rho^{\text{ex}}$  as functions of the intersection parameters (8) are available but omitted here due to space limitations. We also note that although there has been a rich literature on vehicle path planning [40], the above path model is simple and sufficient for our purpose.

Based on the path model (10) and the assumption that a vehicle can follow its pre-planned path perfectly, the dynamic behavior of a vehicle can be characterized using the following

<sup>4</sup>The origin lane and the target lane of a vehicle are, respectively, the lane in which it is driving before entering the intersection and the lane to which it is going after exiting the intersection.

<sup>5</sup>So we have named the intersection entrance (resp. exit) point as  $(x(\rho^{\text{en}}), y(\rho^{\text{en}}))$  (resp.  $(x(\rho^{\text{ex}}), y(\rho^{\text{ex}}))$ ) in the first place.

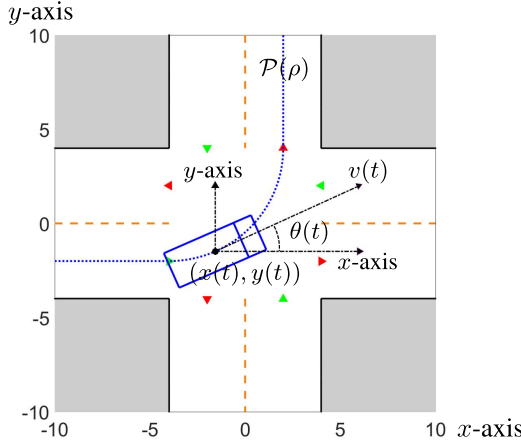


Fig. 3. Vehicle kinematics modeled by (10)-(13). The blue rectangle represents the vehicle's  $c$ -zone where the end with double lines is the vehicle's front end. The blue dotted curve represents the pre-planned path  $\mathcal{P}$ . The states  $x(t)$ ,  $y(t)$  and  $\theta(t)$  can be computed using the traveled distance along the path  $\rho(t)$  and the path geometry (10). The green triangles represent the intersection entrance points  $(x(\rho^{\text{en}}), y(\rho^{\text{en}}))$  and the red triangles the intersection exit points  $(x(\rho^{\text{ex}}), y(\rho^{\text{ex}}))$ .

equations of motion:

$$\begin{aligned}\rho(t+1) &= \rho(t) + v(t) \Delta t, \\ v(t+1) &= v(t) + a(t) \Delta t,\end{aligned}\quad (11)$$

where  $t$  denotes the discrete time,  $v(t) \in [v_{\min}, v_{\max}]$  and  $a(t)$  denote the vehicle's speed and acceleration at  $t$ , and  $\Delta t$  is the sampling period.

Using (10), the vehicle's location  $(x, y)$  and heading angle  $\theta$  can be written as functions of  $\rho$ . In particular,

$$\begin{aligned}\theta(\rho) &= \lim_{h \rightarrow 0^+} \arctan 2(y(\rho + h) - y(\rho), x(\rho + h) - x(\rho)) \\ &= \arctan 2\left(\frac{dy}{d\rho}, \frac{dx}{d\rho}\right).\end{aligned}\quad (12)$$

Then, we collect all relevant variables and define the state of a vehicle as the following 8-tuple,

$$\begin{aligned}s(t) = (\mathcal{P}, \rho(t), v(t), x(\rho(t)), y(\rho(t)), \theta(\rho(t)), \\ \Delta\rho^{\text{en}}(t), \Delta\rho^{\text{ex}}(t)).\end{aligned}\quad (13)$$

Fig. 3 illustrates the vehicle kinematics modeled according to (10)-(13) at a typical two-lane four-way intersection.

To adjust speeds along the path, we assume that a vehicle has a finite set of acceleration levels to choose and apply at each time step, i.e.,

$$a(t) \in A = \{a^1, \dots, a^M\}, \quad \forall t. \quad (14)$$

Incorporating with the above parameterized intersection and vehicle kinematics models, we now rephrase the leader-follower role assignment logic in Section II-A as Algorithm 1.

In Algorithm 1,  $\delta \geq 0$  is a threshold for differentiating the distances, accounting for the fact that human drivers can only estimate the distances with limited accuracy. In particular, we assume that drivers cannot recognize which distance is

---

**Algorithm 1** Leader-follower role assignment

---

**Input** : an ordered pair of vehicles  $(i, j)$  and their states  $(s_i(t), s_j(t))$   
**Output**: whether  $i$  is the leader of  $j$

- 1 **if**  $(\Delta\rho_i^{\text{en}}(t) \leq 0 \text{ and } \Delta\rho_j^{\text{en}}(t) \leq 0) \text{ and } \Delta\rho_i^{\text{ex}}(t) < \Delta\rho_j^{\text{ex}}(t) - \delta$  **then**  $i \prec j$ ;;
- 2 **else if**  $(\Delta\rho_i^{\text{en}}(t) > 0 \text{ or } \Delta\rho_j^{\text{en}}(t) > 0) \text{ and } \Delta\rho_i^{\text{en}}(t) < \Delta\rho_j^{\text{en}}(t) - \delta$  **then**  $i \prec j$ ;;
- 3 **else if**  $i$  and  $j$  are coming from adjacent ways and  $i$ 's way is on the right of  $j$ 's way **then**  $i \prec j$ ;;
- 4 **else if**  $i$  is going straight and  $j$  is making a turn **then**  $i \prec j$ ;;
- 5 **else**  $i \succeq j$ .

---

smaller when  $|\Delta\rho_i^{\text{en}}(t) - \Delta\rho_j^{\text{en}}(t)| \leq \delta$  (resp.  $|\Delta\rho_i^{\text{ex}}(t) - \Delta\rho_j^{\text{ex}}(t)| \leq \delta$ ). According to Algorithm 1, at most one of the outcomes  $i \prec j$  and  $j \prec i$  can take place. It may happen that  $i \succeq j$  and  $j \succeq i$ . In such a case, both vehicles view themselves as followers and thus make conservative decisions. In line 4, “going straight” and “making a turn” need to be differentiated, which is determined according to the angle between the vehicle's origin and target road arms. In particular, when the clockwise angle from its origin road arm to its target road arm is in the interval  $(0, 3\pi/4]$ , the vehicle is “making a left turn”; when the angle is in the interval  $(3\pi/4, 5\pi/4)$ , the vehicle is “going straight”; it is “making a right turn” otherwise.

### C. Driver Reward Function

Basic goals of a driver at an intersection include: 1) to maintain *safety*, e.g., not have a collision with another vehicle, 2) to keep a reasonable distance from other vehicles to improve safety and comfort, and 3) to pass through the intersection and get to his/her target lane under traffic rules and in a timely manner (referred to as *liveness*).

We assume that common traffic rules such as a left turn can only be made when the vehicle is entering the intersection from a left-turn lane (usually the leftmost forward lane), as well as speed limits, have been incorporated in path planning and speed bounds  $v(t) \in [v_{\min}, v_{\max}]$ . Then, the other goals can be represented using a reward function as follows:

$$\mathbb{R}(t) = \sum_{\tau=1}^N \lambda^{\tau-1} R(\tau|t), \quad (15)$$

where  $R(\tau|t)$  is a prediction of the stage reward at time step  $t + \tau$  with the prediction made at the current time  $t$ ,  $N$  is the prediction horizon, and  $\lambda \in [0, 1]$  is a factor discounting future rewards. In particular, the stage reward is defined as a linear combination of three terms, each of which represents a goal introduced above, as follows:

$$R(\tau|t) = w_1 \hat{c}(\tau|t) + w_2 \hat{s}(\tau|t) + w_3 \hat{v}(\tau|t), \quad (16)$$

where  $w_i > 0$ ,  $i \in \{1, 2, 3\}$ , are weighting factors, and the terms  $\hat{c}(\tau|t)$ ,  $\hat{s}(\tau|t)$  and  $\hat{v}(\tau|t)$  are further explained below.

Note that when evaluating actions according to the decision-making model (7), a vehicle considers its interactions with

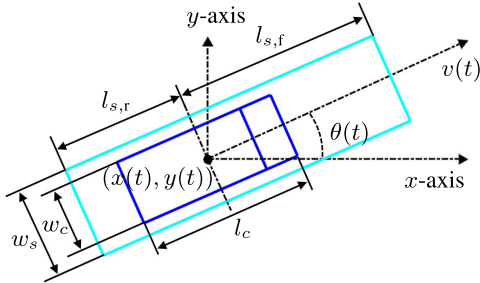


Fig. 4. The  $c$ -zone (dark blue rectangle) and  $s$ -zone (light blue rectangle) of a vehicle.

each of the other vehicles separately. Let  $i$  denote the ego vehicle and  $j$  denote another vehicle in pairwise interactions with  $i$ .

- Collision avoidance,  $\hat{c}$ :

$$\hat{c}(\tau|t) = -(1 + S_c(\tau|t) + \hat{w}|v_i(\tau|t)v_j(\tau|t)|) \mathbb{I}(S_c(\tau|t) > 0),$$

where  $S_c(\tau|t) \geq 0$  is a prediction of the overlapping area between vehicle  $i$  and  $j$ 's  $c$ -zones,  $v_i(\tau|t)$  and  $v_j(\tau|t)$  are the predicted speeds of vehicle  $i$  and  $j$ ,  $\hat{w} > 0$  is a tunable parameter, and  $\mathbb{I}(\cdot)$  is an indicator function taking 1 if  $(\cdot)$  holds and 0 otherwise. The  $c$ -zone of a vehicle has been defined at the beginning of Section III-B, which is a rectangle characterized by the 5-tuple  $(x, y, \theta, l_c, w_c)$ . Thus,  $S_c(\tau|t)$  is determined by the predicted states of vehicle  $i$  and  $j$ , i.e.,  $S_c(\tau|t) = S_c(s_i(\tau|t), s_j(\tau|t))$ .

The term  $\hat{c}$  is designed as above so that when  $S_c(\tau|t) = 0$ , i.e., there is no danger of collision,  $\hat{c}(\tau|t) = 0$ ; when  $S_c(\tau|t) > 0$ , i.e., there is a danger of collision, the penalty depends on the overlapping area of  $c$ -zones and the vehicle speeds. In particular, larger penalties are imposed for larger  $S_c$  values and for larger absolute values of  $v_i$  and  $v_j$  as both of them imply more severe collisions; the parameter  $\hat{w} > 0$  adjusts the relative contribution to severity of overlapping area versus speeds; and the addition of 1 ensures a minimum penalty for collisions.

- Separation,  $\hat{s}$ :

$$\hat{s}(\tau|t) = -(1 + S_s(\tau|t) + \hat{w}|v_i(\tau|t)v_j(\tau|t)|) \mathbb{I}(S_s(\tau|t) > 0),$$

where  $S_s(\tau|t) \geq 0$  is a prediction of the overlapping area between vehicle  $i$  and  $j$ 's “separation zones” ( $s$ -zones). The  $s$ -zone of a vehicle is defined as a rectangle that shares the same longitudinal line of symmetry with the vehicle's  $c$ -zone and over-bounds the  $c$ -zone with a safety margin (see Fig. 4). It can be characterized by a 6-tuple  $(x, y, \theta, l_{s,f}, l_{s,r}, w_s)$ , where  $l_{s,f}, l_{s,r} \geq l_c/2$  and  $w_s \geq w_c$ . In particular, when the ego vehicle  $i$  is the leader (resp. the follower) in the pairwise interaction with vehicle  $j$ ,  $i$  assumes that both vehicles have their  $s$ -zones of the same size, denoted by  $(l_{s,f}^l, l_{s,r}^l, w_s^l)$  (resp.  $(l_{s,f}^f, l_{s,r}^f, w_s^f)$ ). We let  $l_{s,f}^l \leq l_{s,f}^f$ ,  $l_{s,r}^l \leq l_{s,r}^f$  and  $w_s^l \leq w_s^f$  to further encourage the leader to take comparatively more aggressive actions than the follower, since in this way the leader pursues a smaller separation distance than that pursued by the follower.

- Velocity,  $\hat{v}$ : We use the ego vehicle's speed along the path to characterize its liveness. In particular, since a higher speed

corresponds to a shorter time to reach the target lane, we let  $\hat{v}(\tau|t) = v_i(\tau|t)$ .

Note that the predicted stage reward (16) depends on the predicted states  $(s_i(\tau|t), s_j(\tau|t))$  of the two vehicles. According to the vehicle kinematics model (10)-(13),  $s_\xi(\tau|t)$ , for  $\xi \in \{i, j\}$ , is uniquely determined by vehicle  $\xi$ 's current state  $s_\xi(t)$  and predicted acceleration sequence  $\{a_\xi(k|t)\}_{k=0}^{\tau-1}$ , i.e.,  $s_\xi(\tau|t) = s_\xi(s_\xi(t), \{a_\xi(k|t)\}_{k=0}^{\tau-1})$ . We define an action  $\gamma_\xi(t)$  of vehicle  $\xi$  at the current time  $t$  as an acceleration sequence  $\{a_\xi(\tau|t)\}_{\tau=0}^{\mathcal{N}-1}$ , taking values in the action set  $\Gamma = A^{\mathcal{N}}$ . Then, the cumulative reward (15) can be written as a function of  $s_{i,j}(t)$ ,  $\gamma_i(t)$  and  $\gamma_j(t)$ , consistent with the expressions in our decision-making model (7).

The closed-loop operation of the vehicles is based on receding-horizon optimization: Once an acceleration sequence  $\gamma_i^*(t) = \{a_i^*(\tau|t)\}_{\tau=0}^{\mathcal{N}-1}$  has been determined according to (7), vehicle  $i$  applies the first acceleration value  $a_i^*(0|t)$  for one time step, i.e.,  $a_i(t) = a_i^*(0|t)$ , updates its states according to (10)-(13), and then repeats the decision-making process (7) at the new time step.

#### IV. ADDITIONAL MODELING CONSIDERATIONS

To model the decision-making processes of human drivers with higher fidelity, we incorporate several additional considerations in our model. They are discussed in this section.

##### A. Courteous Driving

A vehicle is not supposed to interrupt the other vehicles' nominal drives. More specifically, a vehicle should not intentionally choose an action that would cause a collision when the other vehicles maintain their speeds. We account for this by adjusting the action set for each vehicle, i.e., modify the decision-making model (7) according to

$$\gamma_i^*(t) \in \arg \max_{\gamma_i \in \Gamma_i(t)} \underline{Q}_i(\mathbf{s}_{\text{traffic}}(t), \gamma_i), \quad (17)$$

where  $\Gamma_i(t) \subset \Gamma = A^{\mathcal{N}}$  is defined as

$$\begin{aligned} \Gamma_i(t) &:= A_i(t) \times A^{\mathcal{N}-1}, \\ A_i(t) &:= \left\{ a_i(t) \in A \mid a_i(t) \text{ satisfies either} \right. \\ &\quad \forall j \neq i, a_j(t) = 0 \\ &\quad \Rightarrow S_c(s_{i,j}(t+1)) = S_c(s_{i,j}(t), a_i(t), a_j(t)) = 0, \\ &\quad \left. \text{or } a_i(t) = \min\{a \in A\} \right\}. \end{aligned} \quad (18)$$

We note that although collisions have been penalized through the term  $\hat{c}$  in the reward function (15), the modification here acts essentially as imposing hard constraints to the decision-making problem (7), which, as a well-known fact [41], can typically achieve better constraint satisfaction properties than solely through penalties.

##### B. Limited Perception Ranges

Human drivers have limited ranges of visual perception. To account for this, we assume that a driver only considers his/her interactions with the other vehicles that are in a certain

vicinity of his/her own. In particular, we further modify the decision-making model (7) according to

$$\underline{Q}_i(\mathbf{s}_{\text{traffic}}(t), \gamma_i) = \min_{j \in \Omega_i(t)} Q_{i,j}(\mathbf{s}_{i,j}(t), \gamma_i), \quad (19)$$

where  $\Omega_i(t) \subset \{1, \dots, n\}$  is defined as

$$\Omega_i(t) := \left\{ j \in \{1, \dots, n\} \mid j \neq i \text{ and} \right. \\ \left. \sqrt{(x_j(t) - x_i(t))^2 + (y_j(t) - y_i(t))^2} \leq \omega_i \right\}, \quad (20)$$

with  $\omega_i > 0$  representing vehicle  $i$ 's maximum perception distance.

### C. Breakage of Deadlocks via Exploratory Actions

As discussed at the end of Section II-A, in some scenarios cyclic patterns, such as  $i \prec j$ ,  $j \prec k$ ,  $k \prec l$  and  $l \prec i$ , may occur and cause deadlocks – no one decides to enter the intersection or everyone gets stuck in the middle of the intersection.

Such cyclic patterns also exist in real-world traffic. However, human drivers can usually break a deadlock. When a deadlock occurs, we usually observe that one or more human drivers will probe the possibility of going first and such probes can often help the drivers reach an agreement on their orders of passing through the intersection. On the basis of such an observation, we propose a strategy to break deadlocks via random exploratory actions, presented as Algorithm 2.

---

#### Algorithm 2 Breakage of deadlocks via exploratory actions

---

```

Input : the states of all vehicles
         $\mathbf{s}_{\text{traffic}}(t) = (s_1(t), \dots, s_n(t))$  and the
        acceleration choices of all vehicles
         $(a_1(t), \dots, a_n(t))$  obtained based on (7)
Output: the modified acceleration choices of all vehicles
         $(a_1(t), \dots, a_n(t))$ 
1  $\Omega_{\text{conflict}} = \text{Null};$ 
2 for  $i = 1, \dots, n$  do
3   if  $i$  is the first vehicle coming from its origin lane that
      has not exited the intersection ( $\Delta p_i^{\text{ex}}(t) > 0$ ) then add
       $i$  to  $\Omega_{\text{conflict}}$ ;
4 end
5 if  $v_i(t) = 0$  and  $a_i(t) = 0$ ,  $\forall i \in \Omega_{\text{conflict}}$  then
6   for  $i \in \Omega_{\text{conflict}}$  do
7     if  $\{a \in A_i(t) \mid a > 0\} \neq \emptyset$  then
8       reset  $a_i(t)$  based on  $a_i(t) =$ 
          $\begin{cases} \min\{a \in A_i(t) \mid a > 0\}, & \text{with prob. } p_i, \\ 0, & \text{with prob. } 1 - p_i. \end{cases}$ 
9     end
10   end
11 end

```

---

In Algorithm 2, lines 2-4 are used to identify the vehicles that are in conflict. For example, vehicle  $i$  that has exited the intersection is not a vehicle in conflict. As another example,

TABLE I  
PARAMETER VALUES

Variable(s)	Value(s)	Unit	Remarks
$\Delta t$	1	s	sampling period
$[v_{\min}, v_{\max}]$	[0, 5]	m/s	speed range
$A$	$\{-4, -2, 0, 2\}$	$\text{m/s}^2$	{hard brake, decelerate, maintain, accelerate}
$\delta$	0.5	m	threshold for differentiating distances
$\mathcal{N}$	2		prediction horizon
$\lambda$	0.6		discount factor
$w_{1,2,3}, \hat{w}$	$\{100, 5, 1\}, \frac{1}{4}$		reward function weights
$(l_c, w_c)$	(6, 2.4)	m	c-zone size
$(l_{s,f}^l, l_{s,r}^l, w_s^l)$	(5, 4, 2.8)	m	s-zone size for leader
$(l_{s,f}^f, l_{s,r}^f, w_s^f)$	(14, 4, 2.8)	m	s-zone size for follower
$\forall i \in \{1, \dots, n\}$	30	m	maximum perception distance
$\forall i \in \{1, \dots, n\}$	0.25		probing movement probability

if there is a vehicle  $j$  that is entering/has entered the intersection from the same lane as  $i$ , drives in front of  $i$ ,<sup>6</sup> and has not exited the intersection, then vehicle  $i$  is not a vehicle in conflict. Line 5 is used to identify the occurrence of a deadlock, i.e., all of the vehicles in conflict have stopped and no one decides to move according to decisions of (7). Then, lines 6-10 assign the vehicles in conflict positive probabilities of making slight movements to probe the possibility of going first.

The effectiveness of Algorithm 2 in breaking deadlocks will be illustrated through simulation case studies in Section V.

## V. SIMULATION CASE STUDIES

In this section, we illustrate the proposed game-theoretic framework for modeling the interactive behavior of vehicles at uncontrolled intersections through multiple simulation case studies.

Table I collects all parameters of the framework and their values. These parameter values are manually tuned through a few simulation runs to generate reasonable behavior of the vehicles and then used for all of the simulation case studies in this section including the statistical evaluations. Alternatively, they can be calibrated using a data-driven approach as in [42] or optimized using a simulation-based approach as in [43], and this is left to our future work.

### A. Case Study 1: Reproducing Real-World Traffic Scenarios

We first show that the proposed model can reproduce real-world traffic scenarios. The scenarios are extracted from the video dataset used in [44]. We note that although the traffic

<sup>6</sup>There shall be no ambiguity in “in front of” here since  $i$  and  $j$  are entering/have entered the intersection from the same lane.

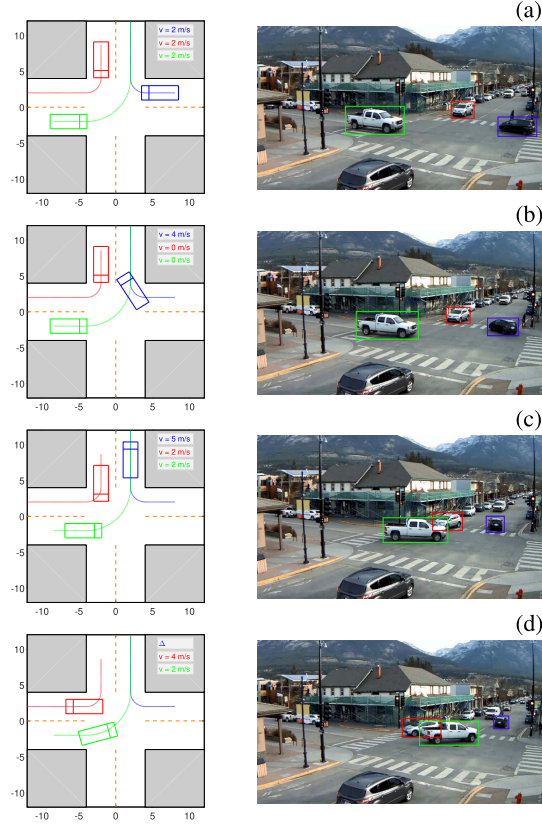


Fig. 5. Reproducing real-world traffic scenario with 3 interacting vehicles by the proposed model.

data are collected at a signalized intersection in Canmore, Alberta, we consider only the vehicles that are legally allowed to enter the intersection (i.e., under a green light or making a right turn), the behavior of which can be modeled similarly to that at uncontrolled intersections. In particular, we initialize the vehicles in our simulation according to the positions and velocities of the corresponding vehicles in the video, and compare the evolution of the scenario simulated using our model to that provided by the video.

Some key frames for a scenario involving 3 interacting vehicles are shown in Fig. 5 and those for a scenario involving 4 interacting vehicles are shown in Fig. 6. It can be observed that our model reproduces both scenarios with satisfactory accuracy. In particular, in both cases the orders in which the interacting vehicles pass through the intersections are predicted correctly by our model and the time-dependent positions of those vehicles predicted by our model match closely to the video data.

#### B. Case Study 2: Completely Symmetric Scenarios

As discussed at the end of Section II-A and at the beginning of Section IV-C, one type of challenging scenarios at uncontrolled intersections for both human drivers and autonomous vehicles are scenarios where no one has a determinable role of leader. Among these scenarios, the ones where all the vehicles arrive at the entrances of a geometrically symmetric intersection at the same time with the same speed may be particularly

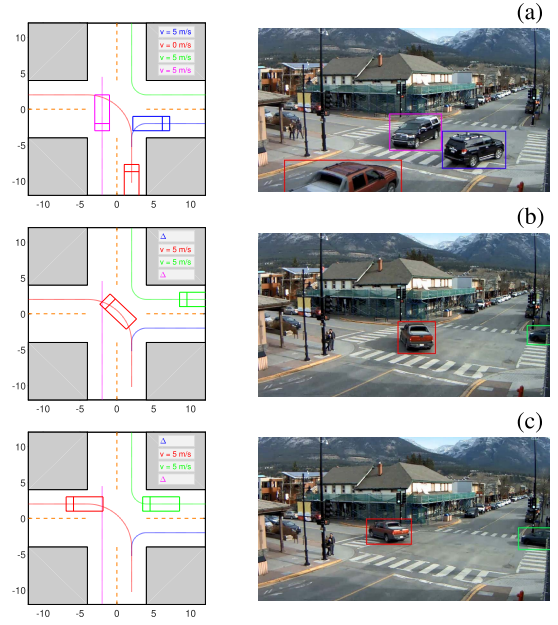


Fig. 6. Reproducing real-world traffic scenario with 4 interacting vehicles by the proposed model.

challenging. In this section, we show the simulation results of two such ‘‘completely symmetric’’ cases.

Both cases involve a geometrically symmetric four-lane (two for each direction) four-way intersection. In the first case, 8 vehicles are approaching the entrances of the intersection from each of the eight forward lanes with the same initial distance  $\Delta\rho^{\text{en}}(0)$  to their corresponding entrance points and the same initial speed  $v(0)$ . Their target lanes all correspond to going straight to cross the intersection. In the second case, 4 vehicles are approaching the entrances of the intersection from each of the four leftmost forward lanes of the road arms with the same  $\Delta\rho^{\text{en}}(0)$  and  $v(0)$ . Their target lanes all correspond to making left turns. In both cases, all of the vehicles are using the model (7) to make initial decisions equipped with Algorithm 2 to handle deadlocks. The simulation results are shown in Figs. 7 and 8.

In Fig. 7(a), the eight vehicles arrive at the entrances of the intersection at the same time. According to Algorithm 1, none of them hold an overall leader role (being the leader in every pairwise interaction). As a result, all of them stop at the intersection entrances to yield (Fig. 7(b)). Then, a deadlock is detected and the blue vehicle makes a probing acceleration according to Algorithm 2 (Fig. 7(c)). After that, the symmetry is broken – the blue vehicle becomes the overall leader and crosses the intersection first (Fig. 7(d)). The other vehicles cross the intersection in a clockwise order (Figs. 7(e)(f)). In Fig. 8(a), after the four vehicles arrive and stop at the intersection entrances, the left purple vehicle makes a probing acceleration and reaches its target lane first (Fig. 8(b)). Similar to Fig. 7, the other vehicles then pass through the intersection in a clockwise order (Figs. 8(c)(d)).

From the above results we can observe that the proposed model exhibits reasonable behavior expected in traffic and has

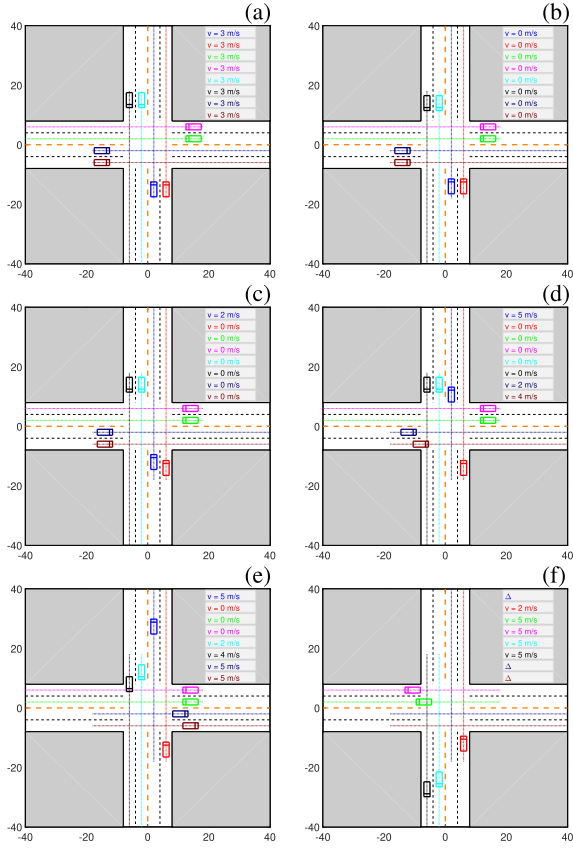


Fig. 7. Completely symmetric case 1. Figures (a-f) show simulation snapshots at a series of sequential steps.

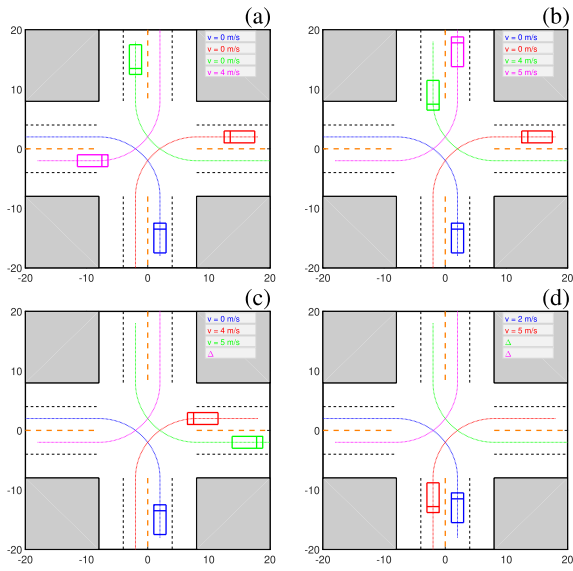


Fig. 8. Completely symmetric case 2. Figures (a-d) show simulation snapshots at a series of sequential steps.

good capability in resolving traffic conflicts in challenging scenarios. We note that there is no centralized control or management in our model to guide the vehicles to resolve their conflicts – the vehicles make their decisions independently. In particular, when a deadlock occurs, the vehicles resolve it through exploratory movements. This is consistent with the

way in which human drivers appear to make decisions and resolve deadlocks in real-world traffic.

### C. Case Study 3: Leader-Follower Model Versus Adaptive Level- $k$ Model

Human drivers can usually resolve traffic conflicts even when they are interacting with other drivers whose driving styles are a priori unknown. A model representing human-driver decision-making processes is supposed to have reasonable robustness against uncertainties in the behavior of interacting drivers. To test such robustness of the proposed model (7), we let vehicles that make decisions according to (7) interact with an alternative model, proposed in our previous work [31], [32] and based on level- $k$  theory [29], [30]. In particular, this alternative model predicts the actions of other vehicles by modeling them as level- $k$  reasoners for  $k \in \{0, 1, \dots, k_{\max}\}$ , adjusts the  $k$  values and the predictions in real time according to observed trajectories, and adapts its own decision strategy to optimally respond to these predictions. This model is termed “adaptive level- $k$  model” and the reader is referred to [31], [32] for further details. We note that this alternative model does not explicitly account for the right-of-way rules or the leader-follower relationships among vehicles, and thus, may not yield to another vehicle that is supposed to have the right of way.

We initialize a three-vehicle interaction scenario as shown in Fig. 9(a). At first, we let the blue vehicle make decisions according to (7) and let the red and green vehicles make decisions according to the alternative model. The corresponding simulation results are shown in the left column of Fig. 9. Then, we switch the models for the blue vehicle and for the red and green vehicles, and the corresponding simulation results are shown in the right column of Fig. 9.

For the former case where the blue vehicle uses (7), since according to Algorithm 1 the blue vehicle is the overall follower, it yields to both the red and green vehicles. For the latter case where the red and green vehicles use (7), since according to Algorithm 1 the green vehicle is the overall leader, it proceeds ahead to cross the intersection first. This shows that our model (7) is not conservative when it has the right of way. Differently from the former case, this time the blue vehicle decides to enter the intersection ahead of the red vehicle. This happens because after the red vehicle yields to the green vehicle, the blue vehicle using the adaptive level- $k$  model thinks that the red vehicle has a conservative driver and thus decides to proceed ahead. Although the red vehicle is supposed to have the right of way over the blue vehicle when they arrive at the entrances of the intersection, it decides to wait until the blue vehicle passes. This shows that our model (7) can respond to changing situations quickly and effectively.

The above results illustrate the robustness of the proposed model (7) for interacting with uncertain drivers.

### D. Case Study 4: Randomized Traffic Scenarios

To comprehensively evaluate the proposed framework, we run a batch test. In particular, we consider intersection scenarios for each fixed number of road arms  $N \in \{3, 4, 5\}$

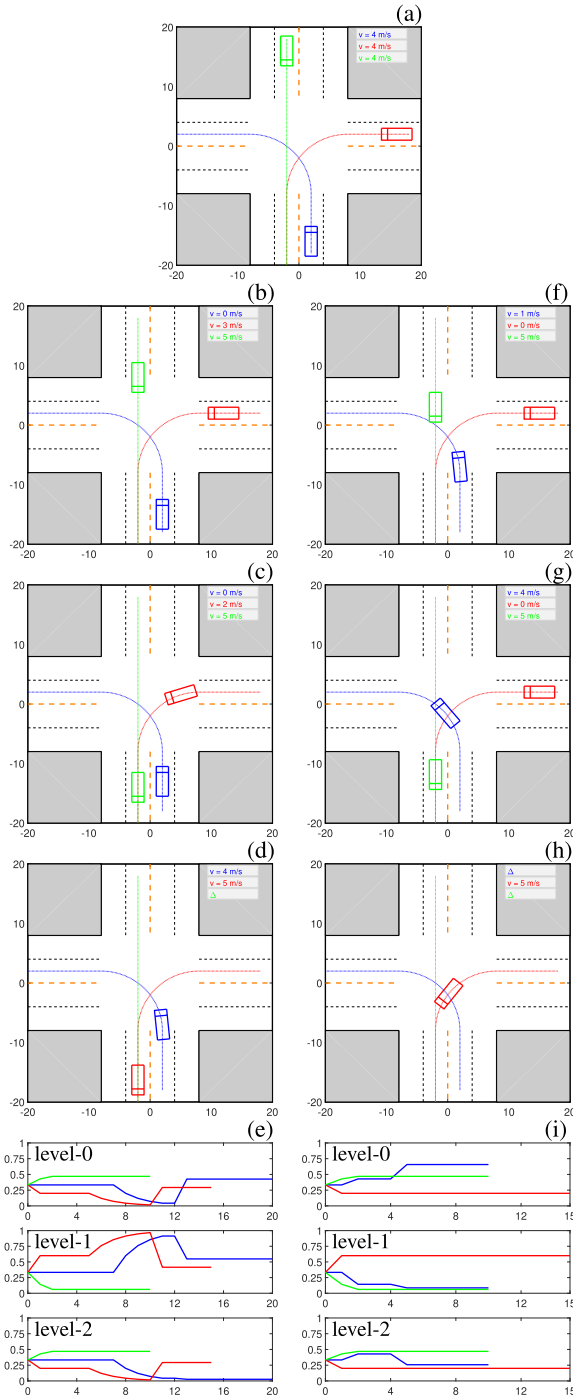


Fig. 9. Leader-follower model versus adaptive level-k model. Left: the blue car makes decisions according to (7) and the other two cars according to the adaptive level-k model in [31], [32]. Right: the blue car makes decisions according to the adaptive level-k model and the other two cars according to (7). Panels (e) and (i) show the time histories of the level estimates for the three vehicles in the adaptive level-k model (see [31], [32] for details).

and each fixed number of vehicles  $n \in \{2, 4, 6, 8, 10\}$  but with randomized layout and geometry parameters  $\{M_f^{(m)}\}_{m=1}^N$ ,  $\{M_b^{(m)}\}_{m=1}^N$  and  $\{\phi^{(m)}\}_{m=1}^N$  and randomized initial conditions including the origin and target lanes, initial distances to intersection entrances  $\Delta\rho^{\text{en}}(0)$  and initial speeds  $v(0)$  of the vehicles.

In particular, we sample  $\{M_f^{(m)}\}_{m=1}^N$  and  $\{M_b^{(m)}\}_{m=1}^N$  based on categorical distributions and  $\{\phi^{(m)}\}_{m=1}^N$  based on truncated normal distributions<sup>7</sup> as follows:

$$M_\xi^{(m)} \sim \text{Cat}\left(\{1, 2, 3\}, \{0.15, 0.7, 0.15\}\right), \quad \xi \in \{f, b\},$$

$$\phi^{(m)} \sim \text{Normal}\left(\frac{2m\pi}{N}, \frac{\pi}{24}, \left[\frac{2m\pi}{N} - \frac{\pi}{8}, \frac{2m\pi}{N} + \frac{\pi}{8}\right]\right).$$

Once the intersection has been created, we assign each vehicle's origin road arm based on a uniform distribution over all road arms, and assign its origin lane based on a uniform distribution over all forward lanes of its origin road arm. After that, we assign its target road arm and target lane based on uniform distributions over, respectively, all acceptable road arms and all acceptable backward lanes of the assigned target road arm, where “acceptable” means satisfying common traffic rules such as a left turn can only be made when the vehicle is entering the intersection from the leftmost forward lane. Then, each vehicle's  $\Delta\rho^{\text{en}}(0)$  and  $v(0)$  are initialized based on uniform distributions over the ranges [10, 28] [m] and [2, 4] [m/s]. Furthermore, we enforce a minimum initial separation  $\rho^{\text{sep}}$  between any two vehicles that are initialized in the same origin lane – if  $\Delta\rho_i^{\text{en}}(0)$  of vehicle  $i$  is in the range of  $[\Delta\rho_j^{\text{en}}(0) - \rho^{\text{sep}}, \Delta\rho_j^{\text{en}}(0) + \rho^{\text{sep}}]$  for any vehicle  $j$  that has been initialized before vehicle  $i$  and is in the same origin lane of vehicle  $i$ , then  $\Delta\rho_i^{\text{en}}(0)$  is re-sampled as above.

We run 100 simulations for each pair of  $(N, n)$ . Some of the simulated traffic scenarios are shown in Fig. 10.

1) *Statistical Evaluation*: We define three metrics to evaluate the proposed framework for modeling the interactive behavior of vehicles at uncontrolled intersections in terms of safety and liveness, including the rate of success (SR), the rate of collision (CR) and the rate of deadlock (DR). The rate of success is defined as the proportion of simulation runs where all of the vehicles safely (without colliding with any other vehicles) reach their terminal points  $(x^{\text{term}}, y^{\text{term}})$  within 60 [s] of simulation time. The rate of collision is defined as the proportion of simulation runs where at least one vehicle collision occurs (once a vehicle collision occurs at a simulation step, the simulation run stops at that step). The rate of deadlock is defined as the proportion of simulation runs where no vehicle collision occurs but there is at least one vehicle that does not reach its terminal point  $(x^{\text{term}}, y^{\text{term}})$  within 60 [s] of simulation time. We note that based on their definitions,  $\text{SR} + \text{CR} + \text{DR} = 1$ . A model representing human-driver decision-making processes is supposed to have reasonably high SR, and reasonably low CR and DR. The evaluation results of our model are shown in Fig. 11.

It can be observed that as the numbers of road arms and of vehicles increase, corresponding to traffic scenarios of increased complexity, the CR and DR also increase. In three-way and four-way intersection scenarios with 2 or 4 vehicles, no collisions or deadlocks are observed. When up to 10 vehicles are interacting at three-way or four-way intersections, the SRs are higher than 0.9. It can also be observed that five-way intersections are more challenging (with higher CR

<sup>7</sup> with mean  $\frac{2m\pi}{N}$  and standard deviation  $\frac{\pi}{24}$  truncated to the range  $[\frac{2m\pi}{N} - \frac{\pi}{8}, \frac{2m\pi}{N} + \frac{\pi}{8}]$ .

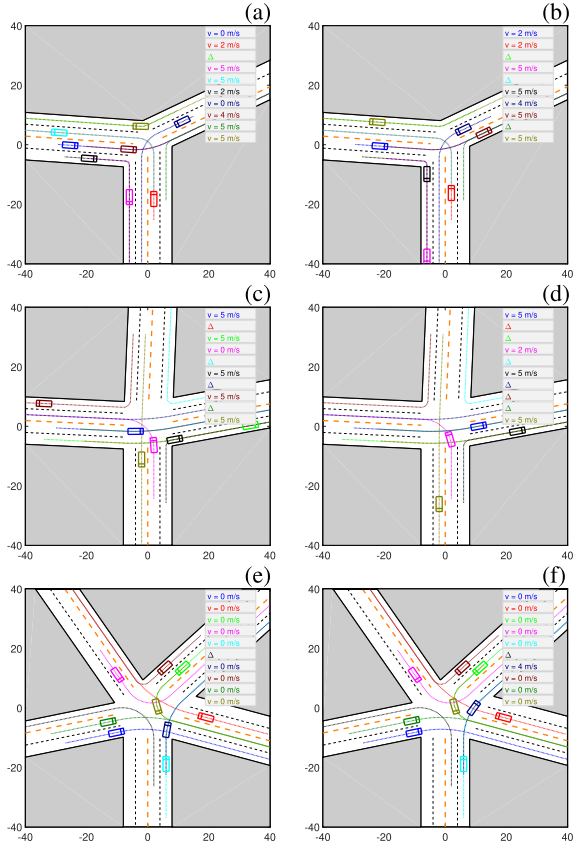


Fig. 10. Randomized traffic scenarios at randomized intersections. Figures (a-b) show simulation snapshots at two sequential steps in a three-way intersection scenario, figures (c-d) show those in a four-way intersection scenario, and figures (e-f) show those in a five-way intersection scenario.

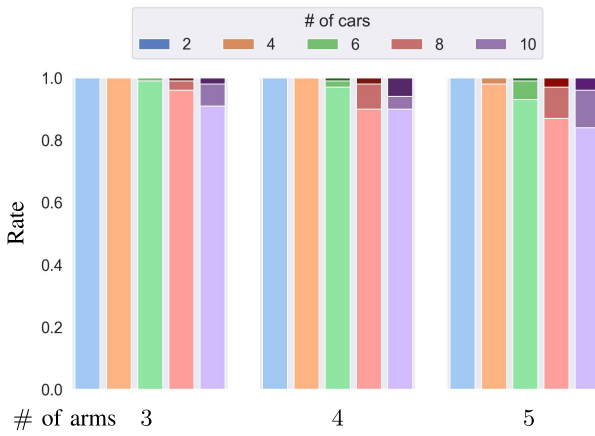


Fig. 11. Statistical evaluation of the vehicle interaction model. Light color: SR, medium color: DR, dark color: CR.

and DR compared to three-way and four-way intersections), where the SR drops to 0.84 for the case of 10 interacting vehicles. This happens because five-way intersections allow more vehicles to arrive at the intersection entrances or be inside the intersection at the same time compared to three-way and four-way intersections, which may cause higher chances of traffic conflicts. Indeed, five-way intersections are also more

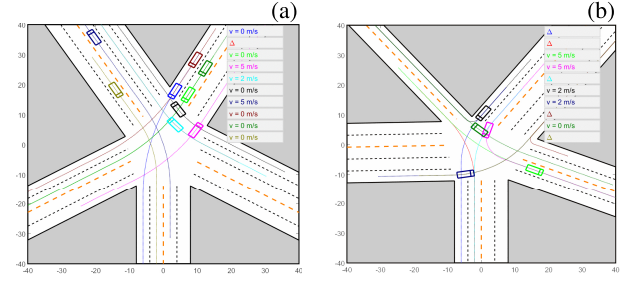


Fig. 12. Two failure cases. (a) A deadlock scenario. (b) A collision scenario.

challenging to human drivers compared to three-way and four-way intersections in real-world traffic.

Furthermore, by looking into the simulation runs with collisions, we find that most collisions are caused by simultaneous exploratory actions of two or more vehicles in deadlock scenarios. Note that in Algorithm 2, a vehicle is not permitted to accelerate if its acceleration would cause a collision when the other vehicles in conflict remain stopped. However, if two or more vehicles accelerate at the same time, it is possible that their simultaneous accelerations cause a collision though each single acceleration would not. Two of the failure scenarios are shown in Fig. 12.

Note that in our simulation results we observe higher collision and deadlock rates than observed in real-world traffic, especially for larger numbers of interacting vehicles. Even so, we note that modeling human driver behavior, especially for multi-vehicle interaction scenarios, is a difficult and open problem, and our results are comparable with several other approaches proposed in the literature for modeling multi-vehicle interactions at uncontrolled intersections. For instance, for four-way intersection with 4 interacting vehicles, the approach of [45] leads to a series of collision rates ranging from 0% to 1.1% and a series of deadlock rates ranging from 0% to 14.3% depending on the simulation settings; while our framework has constant 0% collision rate and 0% deadlock rate for randomized settings. For four-way intersection with 2 to 6 interacting vehicles, the approach of [20] achieves collision-free simulations, at the cost of a rapid increase in the number of deadlocks with the increase in the number of interacting vehicles. In particular, when the number of interacting vehicles increases to 6, almost 50% simulation runs following the approach of [20] end up with deadlocks. In contrast, for four-way intersection with 6 interacting vehicles, our framework has 1% collision rate and 2% deadlock rate.

We remark that our results are associated with a more complex intersection model (see Section III-A) than the four-way intersections considered in [20] and [45]. For example, unlike our intersection model where the angles between road arms and the number of lanes for each road arm can vary, [20] and [45] run their simulation experiments on a simple two-lane (one for each direction) four-way intersection model with orthogonal road arms. Since the scenarios generated by our intersection model are more complex, they can be more challenging for the vehicles to navigate. Meanwhile, simulation results for these more complex scenarios can provide

more insight into interactive vehicle behavior. We also remark that the collision and deadlock rates of our framework can be adjusted through tuning the weights of different terms in the reward function (16). For instance, it may be possible to reduce the number of collisions, which are more severe failures, by increasing the weights  $w_1, w_2$  for collision avoidance and separation, at the cost of a larger number of deadlocks, which are less severe. However, this may not be desirable for our intended use case of the developed traffic model for virtual testing of autonomous vehicle control systems. This is because a traffic model with a low collision rate but a high deadlock rate may tend to be overly conservative and less likely to generate challenging test scenarios for the autonomous vehicles. Nevertheless, we note that developing improvements to the proposed modeling framework to reduce its collision and deadlock rates to a more realistic level represents an opportunity for continuing research and will be pursued in future work.

For the vehicles that safely reach their terminal points within 60 [s] of simulation time, we count their average completion time (CT), which is defined as the duration (in [s] of simulation time) from the simulation initialization to the time instant when the vehicle reaches its terminal point. The average CT can reflect how conservative the decision-making model is. The average CTs for different numbers of road arms and vehicles are shown in Fig. 13.

It can be observed that as the numbers of vehicles increase, the vehicles need more time to pass through the intersections. In particular, for the cases of 2 and 4 interacting vehicles, the average CTs exhibited by our model correspond to level-B in the traffic quality rating system called the “level-of-service” (LOS) for unsignalized intersections defined based on the average control delay [46]. LOS-B corresponds to traffic with a high degree of freedom and a small amount of interactions and is characterized by 10-15 [s] of average control delay [47]. For the cases of 6-10 interacting vehicles, the average CTs exhibited by our model correspond to LOS-C, which corresponds to traffic with restricted freedom due to significant interactions and is characterized by 15-25 [s] of average control delay. Furthermore, among three-, four- and five-way intersections, the vehicles spend the least times to pass through four-way intersections. This is consistent with the observation that the right-of-way traffic rules appear to function best for four-way intersections, which, as a matter of fact, are most common in real-world road networks.

**2) Computational Complexity:** In addition to the rate of success and the average completion time we are also concerned about the computational complexity of the proposed framework, as it determines the scalability of the framework for modeling intersection scenarios with increased complexity. As mentioned in Section II-C, traditional generalizations of leader-follower based game-theoretic models to  $n$ -player settings require exponentially increased computational effort to solve for solutions as the number of players  $n$  increases [37]. However, thanks to the pairwise decoupling of vehicle interactions, the computational complexity of our decision-making model (7) (solved using a tree-search method) increases only linearly as  $n$  increases. We use the average and the worst-case

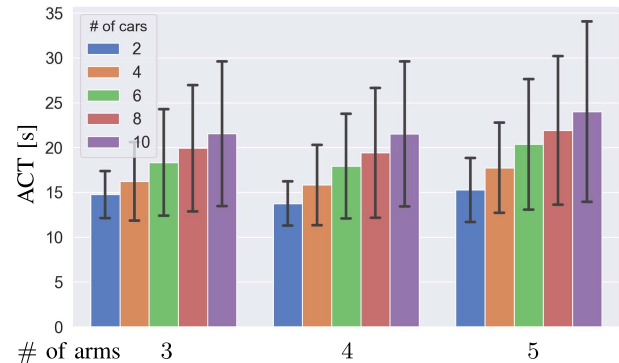


Fig. 13. Average completion time (ACT). The black vertical bars represent the standard deviations.

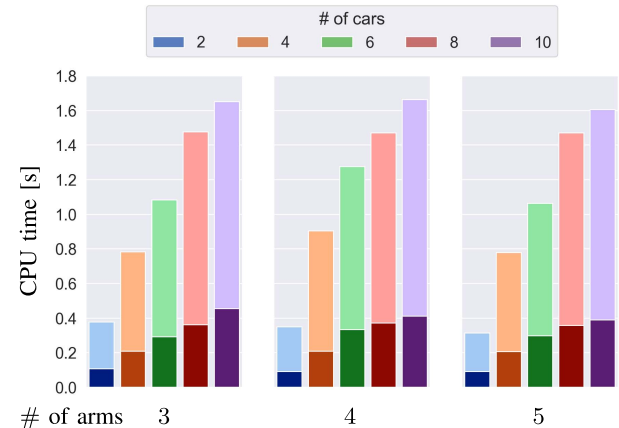


Fig. 14. Average (dark-colored bars) and worst-case (light-colored bars) computation times per vehicle per step.

computation times per vehicle per step (in [s] of real time) to measure our model’s computational complexity, which are the average and the worst-case CPU times for one vehicle to confirm its action choice for one step (including the time to compute the initial action choice using (7) and the time to adjust the action choice using Algorithm 2 if a deadlock is detected). The results for different numbers of road arms and vehicles are shown in Fig. 14. The simulations are performed on Matlab R2016a platform using an Intel Core i7-4790 3.60 GHz PC with Windows 10 and 16.0 GB of RAM. The computation times are calculated using the Matlab *tic-toc* command.

One key observation is that the increase in computation times slows down as the number of vehicles increases. This happens because as the number of vehicles increases, it becomes more likely for the vehicles to be outside of each other’s perception range  $\omega_i$ , and in turn, the actual number of vehicles involved in the computation of solutions for (7) decreases (see Section IV-B). In general, the linear increase in computational complexity and the above observation ensure our framework to have reasonably good scalability for modeling increasingly complex intersection scenarios.

We also remark that the adaptive level-k model in our previous work [31], [32] does not appear to have such a scalability. More detailed discussion on the computational characteristics of the adaptive level-k model is left to future publications.

## VI. SUMMARY

In this article, we proposed a game-theoretic framework for modeling the interactive behavior of vehicles in multi-vehicle uncontrolled intersection scenarios. Our approach takes into account common traffic rules to designate a leader-follower relationship between each pair of interacting vehicles. A model based on pairwise leader-follower relationships is used to represent the interactive decision-making processes of vehicles. Additional modeling considerations, representing courteous driving, limited perception ranges and the capability of human drivers for resolving deadlock scenarios through exploratory actions, are also incorporated in the model.

The interactive decision-making model is integrated with a parameterized intersection model so that interactive traffic in various uncontrolled intersection scenarios (with various numbers of interacting vehicles, intersection layouts and geometries, etc) can be modeled and simulated.

Simulation results showed that the model exhibited reasonable behavior expected in traffic, including the capability of reproducing scenarios extracted from real-world traffic data as well as reasonably high rates of success and realistic average completion times in resolving traffic conflicts. Moreover, thanks to the pairwise decoupling of vehicle interactions, the model has linearly increasing computational complexity as the number of interacting vehicles increases, which improves its scalability.

The framework proposed in this article for modeling multi-vehicle interactions at uncontrolled intersections can be used to formulate a simulation tool for testing, verification, validation and calibration of autonomous driving systems [28], [48], [49].

In addition, with further improvements to reduce the collision and deadlock rates, it may also be utilized in the high-level decision-making algorithms of autonomous vehicles [31], [32], and be exploited to support intersection automation/autonomous intersection management [39]. Moreover, vehicle interactions in some other scenarios, such as highway merging and operation in parking lots, may be modeled based on the proposed framework with modified road layouts and geometries. These are left as topics for future research.

## REFERENCES

- [1] J. M. Anderson, K. Nidhi, K. D. Stanley, P. Sorensen, C. Samaras, and O. A. Oluwatola, *Autonomous Vehicle Technology: A Guide for Policymakers*. Santa Monica, CA, USA: Rand Corporation, 2014.
- [2] M. Buehler, K. Iagnemma, and S. Singh, *The DARPA Urban Challenge: Autonomous Vehicles in City Traffic*, vol. 56. Cham, Switzerland: Springer, 2009.
- [3] N. Kalra. (Mar. 30, 2019). *With Driverless Cars, How Safe is Safe Enough?*. [Online]. Available: <http://www.rand.org/blog/2016/02/with-driverless-cars-how-safe-is-safe-enough.html>
- [4] I. of Transportation Engineers. (2018). *Unsignalized Intersection Improvement Guide*. [Online]. Available: <http://toolkits.ite.org/uig/>
- [5] G. M. Björklund and L. Åberg, "Driver behaviour in intersections: Formal and informal traffic rules," *Transp. Res. F, Traffic Psychol. Behav.*, vol. 8, no. 3, pp. 239–253, 2005.
- [6] M. Liu, G. Lu, Y. Wang, and Z. Zhang, "Analyzing drivers' crossing decisions at unsignalized intersections in China," *Transp. Res. F, Traffic Psychol. Behav.*, vol. 24, pp. 244–255, May 2014.
- [7] G. R. Patil and D. S. Pawar, "Microscopic analysis of traffic behavior at unsignalized intersections in developing world," *Transp. Lett.*, vol. 8, no. 3, pp. 158–166, May 2016.
- [8] NHTS. Administration. (2018). *Fatality Analysis Reporting System*. [Online]. Available: <https://www-fars.nhtsa.dot.gov/>
- [9] D. Carlino, S. D. Boyles, and P. Stone, "Auction-based autonomous intersection management," in *Proc. 16th Int. Conf. Intell. Transp. Syst. (ITSC)*, Oct. 2013, pp. 529–534.
- [10] G. R. de Campos, P. Falcone, and J. Sjoberg, "Autonomous cooperative driving: A velocity-based negotiation approach for intersection crossing," in *Proc. 16th Int. Conf. Intell. Transp. Syst. (ITSC)*, Oct. 2013, pp. 1456–1461.
- [11] M. Ahmene et al., "Modeling and controlling an isolated urban intersection based on cooperative vehicles," *Transp. Res. C, Emerg. Technol.*, vol. 28, pp. 44–62, Mar. 2013.
- [12] K. Dresner and P. Stone, "A multiagent approach to autonomous intersection management," *J. Artif. Intell. Res.*, vol. 31, pp. 591–656, Mar. 2008.
- [13] J. Wu, A. Abbas-Turki, and A. El Moudni, "Cooperative driving: An ant colony system for autonomous intersection management," *Int. J. Speech Technol.*, vol. 37, no. 2, pp. 207–222, Sep. 2012.
- [14] J. Lee and B. Park, "Development and evaluation of a cooperative vehicle intersection control algorithm under the connected vehicles environment," *IEEE Trans. Intell. Transp. Syst.*, vol. 13, no. 1, pp. 81–90, Mar. 2012.
- [15] M. Althoff, O. Stursberg, and M. Buss, "Model-based probabilistic collision detection in autonomous driving," *IEEE Trans. Intell. Transp. Syst.*, vol. 10, no. 2, pp. 299–310, Jun. 2009.
- [16] M. Althoff and J. M. Dolan, "Online verification of automated road vehicles using reachability analysis," *IEEE Trans. Robot.*, vol. 30, no. 4, pp. 903–918, Aug. 2014.
- [17] A. Liniger, A. Domahidi, and M. Morari, "Optimization-based autonomous racing of 1: 43 scale RC cars," *Optim. Control Appl. Methods*, vol. 36, no. 5, pp. 628–647, 2015.
- [18] W. Schwarting, J. Alonso-Mora, L. Paull, S. Karaman, and D. Rus, "Safe nonlinear trajectory generation for parallel autonomy with a dynamic vehicle model," *IEEE Trans. Intell. Transp. Syst.*, vol. 19, no. 9, pp. 2994–3008, Dec. 2017.
- [19] C. You, J. Lu, D. Filev, and P. Tsiotras, "Advanced planning for autonomous vehicles using reinforcement learning and deep inverse reinforcement learning," *Robot. Auto. Syst.*, vol. 114, pp. 1–18, Apr. 2019.
- [20] R. Mandiau, A. Champion, J.-M. Auberlet, S. Espié, and C. Kolski, "Behaviour based on decision matrices for a coordination between agents in a urban traffic simulation," *Int. J. Speech Technol.*, vol. 28, no. 2, pp. 121–138, Apr. 2008.
- [21] D. Sadigh, S. Sastry, S. A. Seshia, and A. D. Dragan, "Planning for autonomous cars that leverage effects on human actions," *Robot., Sci. Syst.*, vol. 2, Jun. 2016.
- [22] M. Bahram, A. Lawitzky, J. Friedrichs, M. Aeberhard, and D. Wollherr, "A game-theoretic approach to replanning-aware interactive scene prediction and planning," *IEEE Trans. Veh. Technol.*, vol. 65, no. 6, pp. 3981–3992, Jun. 2016.
- [23] H. Yu, H. E. Tseng, and R. Langari, "A human-like game theory-based controller for automatic lane changing," *Transp. Res. C, Emerg. Technol.*, vol. 88, pp. 140–158, Mar. 2018.
- [24] A. Dreves and M. Gerdts, "A generalized Nash equilibrium approach for optimal control problems of autonomous cars," *Optim. Control Appl. Methods*, vol. 39, no. 1, pp. 326–342, Jan. 2018.
- [25] R. B. Myerson, *Game Theory*. Cambridge, U.K.: Harvard Univ. Press, 2013.
- [26] D. W. Oyler, Y. Yildiz, A. R. Girard, N. I. Li, and I. V. Kolmanovsky, "A game theoretical model of traffic with multiple interacting drivers for use in autonomous vehicle development," in *Proc. Amer. Control Conf. (ACC)*, Jul. 2016, pp. 1705–1710.
- [27] N. Li, D. Oyler, M. Zhang, Y. Yildiz, A. Girard, and I. Kolmanovsky, "Hierarchical reasoning game theory based approach for evaluation and testing of autonomous vehicle control systems," in *Proc. IEEE 55th Conf. Decis. Control (CDC)*, Dec. 2016, pp. 727–733.
- [28] N. Li, D. W. Oyler, M. Zhang, Y. Yildiz, I. Kolmanovsky, and A. R. Girard, "Game theoretic modeling of driver and vehicle interactions for verification and validation of autonomous vehicle control systems," *IEEE Trans. Control Syst. Technol.*, vol. 26, no. 5, pp. 1782–1797, Sep. 2018.
- [29] R. Nagel, "Unraveling in guessing games: An experimental study," *Amer. Econ. Rev.*, vol. 85, no. 5, pp. 1313–1326, 1995.
- [30] D. O. Stahl and P. W. Wilson, "On players' models of other players: Theory and experimental evidence," *Games Econ. Behav.*, vol. 10, no. 1, pp. 218–254, Jul. 1995.

- [31] N. Li, I. Kolmanovsky, A. Girard, and Y. Yildiz, "Game theoretic modeling of vehicle interactions at unsignalized intersections and application to autonomous vehicle control," in *Proc. Annu. Amer. Control Conf. (ACC)*, Jun. 2018, pp. 3215–3220.
- [32] R. Tian, S. Li, N. Li, I. Kolmanovsky, A. Girard, and Y. Yildiz, "Adaptive game-theoretic decision making for autonomous vehicle control at roundabouts," in *Proc. IEEE 57th Conf. Decis. Control (CDC)*, Dec. 2018, pp. 321–326.
- [33] NHTS. Administration. (2018). *Right-of-Way Rules*. [Online]. Available: <https://one.nhtsa.gov/DOT/NHTSA/NTI/Article/RightOfWay/RightOfWayRules.pdf>
- [34] T. Basar and G. J. Olsder, *Dynamic Noncooperative Game Theory*, vol. 23. Philadelphia, PA, USA: SIAM, 1999.
- [35] H. Von Stackelberg, *Market Structure and Equilibrium*. Cham, Switzerland: Springer, 2010.
- [36] X. Ma and I. Andréasson, "Estimation of driver reaction time from car-following data: Application in evaluation of general motor-type model," *Transp. Res. Rec.*, vol. 1965, no. 1, pp. 130–141, 2006.
- [37] J. Yoo and R. Langari, "A predictive perception model and control strategy for collision-free autonomous driving," *IEEE Trans. Intell. Transp. Syst.*, vol. 20, no. 11, pp. 4078–4091, Nov. 2019.
- [38] P. Kincaid, *The Rule of the Road: An International Guide to History and Practice*. Santa Barbara, CA, USA: Greenwood Press, 1986.
- [39] L. Chen and C. Englund, "Cooperative intersection management: A survey," *IEEE Trans. Intell. Transp. Syst.*, vol. 17, no. 2, pp. 570–586, Feb. 2016.
- [40] W. Schwarting, J. Alonso-Mora, and D. Rus, "Planning and decision-making for autonomous vehicles," *Annu. Rev. Control, Robot., Auto. Syst.*, vol. 1, no. 1, pp. 187–210, May 2018.
- [41] J. Rawlings, D. Mayne, and M. Diehl, *Model Predictive Control: Theory, Computation, and Design*. Madison, WI, USA: Nob Hill Publishing, 2017. [Online]. Available: <https://books.google.com/books?id=MrJctAEACAAJ>
- [42] M. Kuderer, S. Gulati, and W. Burgard, "Learning driving styles for autonomous vehicles from demonstration," in *Proc. IEEE Int. Conf. Robot. Autom. (ICRA)*, May 2015, pp. 2641–2646.
- [43] M. Zhang, N. Li, A. Girard, and I. Kolmanovsky, "A finite state machine based automated driving controller and its stochastic optimization," in *Proc. ASME Dyn. Syst. Control Conf. Amer. Soc. Mech. Eng. Digit. Collection*, Oct. 2017, Art. no. V002T07A002.
- [44] X. Ren, D. Wang, M. Laskey, and K. Goldberg, "Learning traffic behaviors by extracting vehicle trajectories from online video streams," in *Proc. IEEE 14th Int. Conf. Autom. Sci. Eng. (CASE)*, Aug. 2018, pp. 1276–1283.
- [45] S. Pruekprasert, X. Zhang, J. Dubut, C. Huang, and M. Kishida, "Decision making for autonomous vehicles at unsignalized intersection in presence of malicious vehicles," in *Proc. IEEE Intell. Transp. Syst. Conf. (ITSC)*, Oct. 2019, pp. 2299–2304.
- [46] C. A. Quiroga and D. Bullock, "Measuring control delay at signalized intersections," *J. Transp. Eng.*, vol. 125, no. 4, pp. 271–280, Jul. 1999.
- [47] Transportation Research Board, *HCM 2010: Highway Capacity Manual*, 5th ed. Washington, DC, USA: Transportation Research Board, 2000.
- [48] G. Su, N. Li, Y. Yildiz, A. Girard, and I. Kolmanovsky, "A traffic simulation model with interactive drivers and high-fidelity car dynamics," in *Proc. 2nd Conf. Cyber-Phys. Hum. Syst. (COPHS)*, 2018, pp. 440–445.
- [49] N. Li, M. Zhang, Y. Yildiz, I. Kolmanovsky, and A. Girard, "Game theory-based traffic modeling for calibration of automated driving algorithms," in *Control Strategies for Advanced Driver Assistance Systems and Autonomous Driving Functions*. Cham, Switzerland: Springer, 2019, pp. 89–106.



**Nan Li** (Member, IEEE) received the B.S. degree in automotive engineering from Tongji University, Shanghai, China, in 2014, and the M.S. degrees in mechanical engineering and in mathematics from the University of Michigan, Ann Arbor, MI, USA, in 2016 and 2020, respectively, where he is currently pursuing the Ph.D. degree in aerospace engineering. His research interests include constrained control, stochastic control, and application of game theory to multiagent systems.



**Yu Yao** (Member, IEEE) received the B.Eng. degree in aerospace engineering from the Beijing Institute of Technology in 2015 and the M.S. degree in robotics from the University of Michigan in 2017, where he is currently pursuing the Ph.D. degree with the Robotics Institute. His research interests include anomaly detection, action recognition/prediction, and scene understanding and their applications to autonomous vehicles and intelligent transportation systems.



**Ilya Kolmanovsky** (Fellow, IEEE) received the M.S. and Ph.D. degrees in aerospace engineering and the M.A. degree in mathematics from the University of Michigan, Ann Arbor, MI, USA, in 1993, 1995, and 1995, respectively. He is currently a Full Professor with the Department of Aerospace Engineering, University of Michigan. He is named as an inventor on 100 U.S. patents. His current research interests include control theory for systems with state and control constraints and control applications to aerospace and automotive systems. He was a recipient of the Donald P. Eckman Award of the American Automatic Control Council and two IEEE TRANSACTIONS ON CONTROL SYSTEMS TECHNOLOGY outstanding paper awards.



**Ella Atkins** (Senior Member, IEEE) received the B.S. and M.S. degrees in aeronautics and astronautics from MIT and the M.S. and Ph.D. degrees in computer science and engineering from the University of Michigan. She is currently a Professor of Aerospace Engineering with the University of Michigan, where she directs the Autonomous Aerospace Systems Laboratory, and the Associate Director of Graduate Programs for the Robotics Institute. She is the Editor-in-Chief of the AIAA *Journal of Aerospace Information Systems* (JAIS) and the Past-Chair of the AIAA Intelligent Systems Technical Committee. She has served on the National Academy's Aeronautics and Space Engineering Board and pursues research in aerospace and robotic system contingency planning, autonomy, and safety.



**Anouck R. Girard** (Senior Member, IEEE) received the Ph.D. degree in ocean engineering from the University of California at Berkeley, Berkeley, CA, USA, in 2002. She has been with the University of Michigan, Ann Arbor, MI, USA, since 2006, where she is currently an Associate Professor of Aerospace Engineering. She has coauthored the book *Fundamentals of Aerospace Navigation and Guidance* (Cambridge University Press, 2014). Her current research interests include vehicle dynamics and control systems. She was a recipient of the Silver Shaft Teaching Award from the University of Michigan and the Best Student Paper Award from the American Society of Mechanical Engineers.